CERN-TH.6016/91

STRONGLY INTERACTING $W_L'S$ AND $Z_L'S$ AT TEV ENERGIES[1]

Maria J. HERRERO

CERN, CH-1211 Geneva 23, Switzerland

ABSTRACT

In this talk we review some of the recent ideas on the Strongly Interacting Symmetry Breaking Sector of the Standard Model that are based on the use of Chiral Lagrangians and Chiral Perturbation Theory. Some applications of these ideas to the computation of W_LW_L scattering amplitudes at TeV energies are also presented.

CERN-TH.6016/91
February 1991

[1]Talk presented at the First Triangle CERN-JINR-IHEP Workshop. Dubna, USSR, 1-5 October 1990

1 Introduction

Although we still ignore the dynamics triggering the breakdown of the $SU(2)_L \times U(1)_Y$ gauge symmetry down to $U(1)_{em}$ in the Standard Model (**SM**) , there is the general believe that some manifestation of the Symmetry Breaking Sector (**SBS**) must show up at or below the TeV energy domain. The argument goes as follows. If the SBS is weakly interacting with typically a few light modes in the low energy spectrum, as in the SM or in its minimal supersymmetric version with (at least) one ligth Higgs particle, these modes will be produced and studied in present and/or forthcoming colliders. If, in contrast, the SBS is strongly interacting (for instance, the SM with $M_H \geq 1\ TeV$, technicolor models, composite models, etc.) with resonances typically belonging to the TeV domain, the scattering of the Longitudinal components of the Weak Bosons (**LWB**), V_LV_L ($V_L = W_L^{\pm}$ or Z_L), at the TeV energy scale will provide some help in understanding the nature of the SBS [1,2]. This statement may be understood as follows.

In the case of a **Strongly Interacting Symmetry Breaking Sector (SISBS)** the scattering of the LWB at high energies (say for $\sqrt{s} >> M_W$) dominates the scattering of the transverse components. By means of the Equivalence Theorem one knows that by measuring the $V_LV_L \rightarrow V_LV_L$ scattering at high energies what is really being measured is the scattering of the corresponding Nambu-Goldstone bosons and, consequently, the strength of the interactions in the SBS. Finally, it is precisely the energy scale of about 1 TeV where perturbative unitarity in V_LV_L scattering is broken down, meaning that the V_L's self-interactions cannot be treated perturbatively. Other methods must be applied to study these scattering processes. However, no matter what the method be used, the message concerning the phenomenology is clear. There must be a system that is responsible for restoring unitarity in the V_LV_L scattering at the TeV energy scale [3] and, therefore, some mafestation of it will show up at that energy scale. This system could be the Higgs particle itself as in the SM (H), a composite vector boson such as for instance the technirho ($\rho_{TC}^{\pm}$ and ρ_{TC}^{0}) of Technicolour theories , a composite scalar system resembling the Higgs particle , or it could even be a more exotic system with higher isospin and/or spin quantum numbers not even proposed yet. Unfortunately, on the theoretical side there is still no satisfactory working model for the SISBS so that one cannot make definive predictions for the observables to be measured at the next generation colliders as for instance LHC, SSC and CLIC.

Our aim is to study in a general approach, that is, without making any specific assumption "a priori" about the particular dynamics governing the SBS, the most remarkable physical consequences of a SISBS. In particular we are interested in the consequences for V_LV_L scattering at LHC and SSC. Generally speaking, the SISBS hypothesis simply means *the absence of any physical state belonging to the SBS well below 1 TeV other than the LWB themselves.* In that case, the relative low masses of the gauge bosons as compared to the TeV energy domain, where the emerging resonances are expected to occur, may be understood on the basis of an approximate global symmetry of the SBS which is spontaneously broken and the LWB being the associated Nambu-Goldstone bosons. In order to be able to deal with different physical situations for the SISBS we choose the Chiral Lagrangian formalism and the Chiral Perturbation Theory (**ChPT**) techniques [4] that have been

proven to be quite satisfactory in the context of low energy hadron physics. Since the theory of effective Chiral Lagrangians provides a compact and elegant method for dealing with the interactions of the Goldstone modes of any theory, even in the case where the underlying dynamics is not known, we believe it is the most appropriate approach to the problem of a SISBS. Futhermore, only three requirements must be incorporated in this approach: 1) the global symmetry pattern for the building-up of the Chiral Lagrangian must be compatible with the symmetries of the SM, $SU(2)_L \times U(1)_Y \rightarrow U(1)_{em}$, 2) the ρ parameter must be compatible with its experimental value or, in other words, it must be close to one, and, 3) the value of the dimensionful parameter that plays the role of f_π in low energy hadron physics is fixed here to $v = 246GeV$. These three requirements lead us to adopt the following chiral symmetry breaking pattern: $SU(2)_L \times SU(2)_R \rightarrow SU(2)_V$ with $SU(2)_V$ being the so-called custodial symmetry (the identity $\rho = 1$ is, therefore, guarantee) , and $W_L^{\pm}$, Z_L being the three Nambu-Goldstone bosons associated to this global symmetry breaking.

The V_LV_L scattering may, in fact, be described in formal analogy to $\pi\pi$ scattering. In the latter case the isospin symmetry plays the same role as the custodial symmetry does in the former case. More specifically, ChPT gives an expansion of the V_LV_L scattering amplitudes in powers of $s/(4\pi v)^2$ and it is valid in the energy range $M_W << \sqrt{s} << min(4\pi v, M_R)$, with M_R being the mass of the (unknown) lowest resonance belonging to the SISBS. The explicit formulae of these scattering amplitudes to next to leading order in ChPT ($O(s^2)$) were first presented in [5]. The lower limit in this energy region is because of the validity domain of the Equivalence Theorem. The dimensionful parameter controling the expansion in energy powers gives an upper energy bound of $4\pi v \sim 3TeV$. However, there is an extra upper energy bound that is imposed by unitarity and that restricts even more the actual available energy range to ChPT. The V_LV_L scattering amplitudes computed by means of ChPT do not respect unitarity for energies larger than about 1.5 TeV (first ref. in [5]). This is not only a problem in ChPT but also in the SM where it is a well known fact that for a heavy Higgs particle ($M_H \geq 1\ TeV$) the partial wave amplitudes for LWB scattering violate unitarity at about the same energy as mentioned above. This fact persists in the SM when the one loop corrections to the LWB scattering amplitudes are included. Unfortunately, this problem must be faced whenever a comparison with future measurements at LHC and SSC is pretended. The question of getting unitary answers for the scattering amplitudes is treated here by supplementing the Chiral Lagrangian approach with a unitarization prescription (we call it **Unitarized-ChPT**) [6]. In particular when making predictions for SSC and LHC we make the following choices: the Padé approximant method and the K-matrix one.

For a more detailed description of the ChPT approach for V_LV_L scattering see refs. [5], [7] and [8]. Most of the results presented in this talk are contained in [5] and [7].

2 LWB scattering amplitudes in ChPT

Let us assume the following symmetry breaking pattern

$$SU(2)_L \times SU(2)_R \rightarrow SU(2)_{L+R} \tag{2.1}$$

This chiral symmetry (as well as the custodial symmetry) gets explicitly broken once the global subgroup $SU(2)_L \times U(1)_Y$ is gauged by terms proportional to g', the $U(1)_Y$ coupling constant. However, we will not consider here explicit chiral breaking terms. Since our main interest is the study of the most remarkable SISBS signals, we will work within the approximation of neglecting the interactions of electroweak strength, that is, we will take $g, g' = 0$. Equivalently, we will not consider the coupling of the LWB to the transverse modes nor the photon[2].

The starting point is the use of a convenient parametrization for the Goldstone boson fields $w_1(x), w_2(x), w_3(x)$ associated to the symmetry breaking $SU(2)_L \times SU(2)_R \to SU(2)_{L+R}$. This parametrization is given in terms of a unitary matrix field $U(x)$ belonging to the quotient space $SU(2)_L \times SU(2)_R/SU(2)_{L+R}$ and is defined by:

$$U(x) = exp(\frac{i}{v} w_a(x)\sigma^a) \tag{2.2}$$

with $\sigma^a, a = 1,2,3$ being the Pauli matrices, and v is fixed experimentally by the Fermi constant to the value $v = (G_F\sqrt{2})^{-1/2} = 246GeV$.

Under a chiral $SU(2)_L \times SU(2)_R$ transformation the $U(x)$ matrix field transforms as:

$$U(x) \to V_L U(x) V_R^+ \tag{2.3}$$

with $V_L \in SU(2)_L$ and $V_R \in SU(2)_R$.

The most general chiral invariant Lagrangian is a sum of an infinite number of terms with increasing (even) number of derivatives in the $U(x)$ and the $U(x)^+$ fields and with an infinite number of arbitrary parameters. The resulting effective theory of interacting Goldstone bosons from this general Lagrangian is renormalizable in the sense that all the counterterms needed to remove the infinities appearing in the Green functions from loop contributions are already present in the original Lagrangian. The whole point of an expansion in terms of an increasing number of derivatives, or equivalently in terms of increasing powers of the external momenta, is that at low energy only a finite number of terms are important. Here low energy means much lower than the typical parameter scale that controls the chiral expansion of about $4\pi v$. It follows then that keeping just a few terms in the chiral Lagrangian makes sense and the model can be used to parametrize in a consistent way the low energy scattering amplitudes as a function of a finite number of parameters. To a given order in the chiral expansion the inclusion of loop diagrams will generate a scale dependence that is reabsorbed into the definition of the renormalized parameters while the physical amplitudes remain scale independent.

To lowest order in ChPT, $O(p^2)$, where p is a typical external momentum, the chiral Lagrangian is fixed in terms of just one parameter, v, and has the form:

$$\mathcal{L}_0 = \frac{v^2}{4} Tr(\partial_\mu U \partial^\mu U^+). \tag{2.4}$$

To next-to-leading order, $O(p^4)$, two additional terms have to be included which can be written in the form:

$$\mathcal{L}_1 = MTr(\partial_\mu U \partial^\mu U^+) Tr(\partial_\nu U \partial^\nu U^+) + NTr(\partial_\mu U \partial_\nu U^+) Tr(\partial^\mu U \partial^\nu U^+), \tag{2.5}$$

[2]Some phenomenological consequences for LEP physics of the SISBS in ChPT and by taking into account terms with $g, g' \neq 0$ have been recently studied in [9]

with M and N being two dimensionless parameters.

The predictions for the Goldstone boson interactions (or, equivalently, for the LWB) to lowest order are those of $\mathcal{L}_0$ and therefore depend just on v. They lead to the well-known Low Energy Theorems (**LET**) for the LWB scattering amplitudes [10], $T^{LET}(W_L^i W_L^j \to W_L^k W_L^l) \equiv T_{ijkl}^{LET}$ with $i, j, k, l = \pm, 0$:

$$T_{+-+-}^{LET} = -\frac{u}{v^2}\ ,\ T_{+-00}^{LET} = \frac{s}{v^2}\ ,\ T_{0000}^{LET} = 0\ ,\ T_{\pm 0 \pm 0}^{LET} = \frac{t}{v^2}\ ,\ T_{\pm\pm\pm\pm}^{LET} = -\frac{s}{v^2} \tag{2.6}$$

For next order predictions, $O(p^4)$, we use $\mathcal{L} = \mathcal{L}_0 + \mathcal{L}_1$ instead of $\mathcal{L}_0$ and include the one-loop corrections to $\mathcal{L}_0$ that are also of order $O(p^4)$. The explicit formulae for the amplitudes were obtained in [5] by using the dimensional regularization scheme. They are in agreement with the early results by Weinberg and by Gasser and Leutwyler [4] for the $\pi - \pi$ scattering amplitudes to order $O(p^4)$ in the chiral limit.

The LWB amplitudes to $O(p^4)$ are given by:

$$T(W_L^+ W_L^- \to W_L^+ W_L^-) = A(s,t,u) + A(t,s,u)\ ,\ T(W_L^+ W_L^- \to Z_L^0 Z_L^0) = A(s,t,u)$$

$$T(Z_L^0 Z_L^0 \to Z_L^0 Z_L^0) = A(s,t,u) + A(t,s,u) + A(u,t,s)$$

$$T(W_L^\pm Z_L^0 \to W_L^\pm Z_L^0) = A(t,s,u)\ ,\ T(W_L^\pm W_L^\pm \to W_L^\pm W_L^\pm) = A(t,s,u) + A(u,t,s)$$

$$A(s,t,u) = \frac{s}{v^2} + \frac{4}{v^4}(2M_R(\nu)s^2 + N_R(\nu)(t^2+u^2))$$

$$+\frac{1}{(4\pi)^2 v^4}[-\frac{1}{12}(3t^2+u^2-s^2)\log\frac{-t}{\nu^2} - \frac{1}{12}(3u^2+t^2-s^2)\log\frac{-u}{\nu^2} - \frac{1}{2}s^2\log\frac{-s}{\nu^2}] \tag{2.7}$$

The renormalized constants M_R and N_R are defined in terms of the bare ones M and N so as to cancel the divergences appearing because of the one-loop corrections to $\mathcal{L}_0$. It introduces a dependence of M_R and N_R on the renormalization scale parameter ν that can be easily reproduced by demanding the physical amplitudes to be independent of this scale parameter.This gives:

$$M_R(\nu) = M_R(\nu_0) - \frac{1}{12(4\pi)^2}\log\frac{\nu}{\nu_0}$$

$$N_R(\nu) = N_R(\nu_0) - \frac{1}{6(4\pi)^2}\log\frac{\nu}{\nu_0}, \tag{2.8}$$

where ν_0 is again a reference scale which cannot be set to zero.

The model in this form is completely meaningful and depends on two unknown parameters, M_R and N_R, which contain the information relative to the underlying dynamics. The only thing to bear in mind is that the eventual measurement of these parameters will have to be accompanied by the value of the scale ν at which they have been defined. The value of M_R and N_R at any other energy scale ν' then can be obtained by the use of eq. (2.8).

So far, all that has been said is completely general and can be applied irrespective of the underlying theory. The important outcome to learn is that different choices of M_R and N_R at an arbitrary scale ν will describe different physical situations in the symmetry breaking sector of the SM.

3 Scenarios for the SISBS

In order to study the phenomenological implications of a SISBS at LHC and SSC we have considered three scenarios [7] somehow representative of a set of theories with a low energy behaviour governed respectively by the existence of either a scalar resonance ("scalar-dominated theories") or a vector resonance ("vector-dominated theories") in the TeV energy spectrum. These scenarios are: Scaled-QCD, $SU(N_{TC})$ Technicolour and a Higgs-like scenario.

3.1 Scaled-QCD

This scenario is based on transferring the low energy phenomenology of QCD from the energy domain of several hundred MeV to the region of several hundred GeV. The LWB are really the pions of this Scaled- QCD scenario. In particular, the LWB scattering is a replica of the $\pi-\pi$ scattering data (including the broad enhancement in the I=J=0 channel and the appearance of the ρ resonance in the I=J=1 channel) that have been scaled up in energy by a factor of $v/f_\pi = 2600$. We do this rescaling by means of ChPT and by fixing the parameters to the following values:

$$M_R^{Scaled-QCD}(\frac{v}{f_\pi}\nu) = M_R^{QCD}(\nu) \ ; \ N_R^{Scaled-QCD}(\frac{v}{f_\pi}\nu) = N_R^{QCD}(\nu) \qquad (3.1)$$

where M_R^{QCD} and N_R^{QCD} are the parameters of the $O(p^4)$ terms in the chiral Lagrangian of low energy QCD and in the chiral limit. We use here the values obtained in ref.[6] from a fit to the pion-pion data: $M_R^{QCD}(785MeV) = -9\times10^{-4}$ and $N_R^{QCD}(785MeV) = 1.8\times10^{-3}$.

The physical parameters of the ρ-like resonance of this Scaled-QCD scenario are the following: $M_\rho^{Scaled-QCD} = 2TeV$, $\Gamma_\rho^{Scaled-QCD} = 480GeV$.

3.2 $SU(N_{TC})$ Technicolour

In this scenario, $SU(N_{TC})$ Technicolour [11] , we assume there is a vector resonance I=J=1 in the spectrum. Using large N_{TC} arguments one expects the mass of the vector resonance to go like [11] $M_{\rho_{TC}} \approx M_\rho \frac{v}{f_\pi}(\frac{3}{N_{TC}})^{\frac{1}{2}}$, where $M_\rho = 770MeV$. Increasing N_{TC} implies a lighter resonance as compared to the resonance in the Scaled-QCD scenario that would correspond in this context to $N_{TC} = 3$. By assuming that the KSFR relation [12] holds in $SU(N_{TC})$ theories as it (approximately) does in QCD, more specifically $\Gamma_{\rho_{TC}} = \frac{M_{\rho_{TC}}^3}{96\pi v^2}$, then the larger N_{TC} is, the narrower the resonance turns out to be. In this way one can study the experimental possibilities for detecting vector resonances over a wide range of mass values, based on some general assumptions. In particular, the existence of a lighter resonance increases considerably the production rates of $W^\pm Z^0$ pairs and, thus, the observability of these resonances. The way one has to choose M and N in order to reproduce the low energy behaviour of these $SU(N_{TC})$ scenarios is the following one:

$$M_R^{TC}(\frac{v}{f_\pi}(\frac{3}{N_{TC}})^{\frac{1}{2}}\nu) = \frac{N_{TC}}{3}M_R^{QCD}(\nu) \ ; \ N_R^{TC}(\frac{v}{f_\pi}(\frac{3}{N_{TC}})^{\frac{1}{2}}\nu) = \frac{N_{TC}}{3}N_R^{QCD}(\nu) \qquad (3.2)$$

where M_R^{QCD} and N_R^{QCD} are the same QCD parameters as in eq.(3.1).

In order to take into account properly the contribution of the I=J=1 resonance (the technirho as well as the Scaled-QCD-ρ) in the numerical computations for LHC and SSC, we have chosen the Padé unitarization method. The reason is that it provides a resonant behaviour in the I=J=1 channel with the particularity of fulfilling automatically the KSFR relation. In particular, it is known to reproduce very well the $\pi-\pi$ scattering data in the three channels, I=J=0, I=J=1 and I=2,J=0 [13].

In order to study a wide range of signatures we have considered two technicolour scenarios: 1) $M_{\rho_{TC}} = 1.0TeV$, $\Gamma_{\rho_{TC}} = 55GeV$ and 2) $M_{\rho_{TC}} = 1.5TeV$, $\Gamma_{\rho_{TC}} = 185GeV$. They correspond to $N_{TC} = 12$, and $N_{TC} = 5$ respectively.

3.3 Higgs-like

We choose the parameters of the effective Lagrangian to $O(p^4)$, M and N, so as to reproduce the LWB scattering amplitudes in the SM to one-loop order and in the limit $m_H^2 \gg s$ [14]. Thus, we are simulating the effect at low energies of a very heavy Higgs boson in the SM to one-loop level. The way one has to choose the parameters M and N is the following:

$$M_R^{HIGGS}(\nu) = \frac{v^2}{8M_H^2} + \frac{1}{8}(c_1 - \frac{1}{2}c_2) + \frac{1}{12(4\pi)^2}log\frac{M_H}{\nu} \ ; \ N_R^{HIGGS}(\nu) = \frac{c_2}{8} + \frac{1}{6(4\pi)^2}log\frac{M_H}{\nu} \qquad (3.3)$$

where $c_1 = \frac{1}{(4\pi)^2}(\frac{9\pi}{2\sqrt{3}} - \frac{76}{9})$, $c_2 = -\frac{4}{9}\frac{1}{(4\pi)^2}$ and M_H is the renormalized Higgs mass as defined in the first paper of ref.[14][3].

In addition, whenever we use the ChPT amplitudes of this Higgs-like scenario for numerical computations at SSC and LHC a unitarization procedure has been applied. We enphasize that, in their present form, the ChPT amplitudes violate unitarity at about 1.5 TeV [5] and they should not be used without a unitarization prescription for the event rate computation at LHC or SSC [15]. The two unitarization methods used here give partial waves that verify $Im\ a_{IJ} = |a_{IJ}|^2$. Besides, they are characterized by [7]:

** **K-matrix method:** It stops the increase with energy of the a_{IJ} partial waves (particularly the a_{00} partial wave in this Higgs-like scenario) and gives a saturation behaviour.

** **[1,1]-Padé-approximant method:** It also stops the increase with energy of the a_{IJ} partial waves but instead of saturating all of them it develops a resonant behaviour in the a_{00} channel. The scalar resonance S of the Higgs-like scenario shows up at a mass scale which is given by the position of the pole in the unphysical sheet of the $a_{00}^{[1,1]}(s)$ function [16]. More precisely, in the limit of large M_H ($v^2 << s << M_H^2$), M_S is given by the solution to the equation:

$$M_S^2 = \frac{4v^2}{\frac{1}{3}(22c_1 + \frac{1}{4}c_2) + \frac{100}{9(4\pi)^2}log\frac{M_H}{M_S}}. \qquad (3.4)$$

For the numerical computations at SSC and LHC with this Padé method we choose a Higgs-like scenario having the above mentioned scalar resonance at $M_S \sim 1\ TeV$. It is

[3]Notice that the first term in M_R becomes neglegible in the limit of large M_H, $v^2 << s << M_H^2$. In this limit M_H should be interpreted rather as an effective cut-off and not as the mass of a particle

worth mentioning that, as pointed out in [17], the features obtained by the Padé method when applied to the SM case (in particular the appearance of the so called "*Higgs Remnant*" corresponding in our case to the scalar resonance S) are in qualitative agreement with the ones obtained by the large N expansion of the O(N) model [18].

3.4 Comparison of the SISBS scenarios in ChPT

We have computed the numerical values of the parameters in the three scenarios, eqs. (3.1), (3.2) and (3.3). The results are ploted in fig.1 for various choices of M_H, N_{TC} and the energy scale ν.

The most relevant outcome is the fact that the two qualitatively different scenarios, called in this plot Higgs-like and QCD-like, populate different regions of the parameter space (N_R, M_R) and, in consequence, one expects different patterns for the observables that will be predicted from those values. In terms of the more familiar notation of Gasser and Leutwyler in [4] that differs sligthly from the one used in this paper by:

$$M_R(\nu) = \hat{M}_R(\nu) + \frac{1}{36(4\pi)^2} \;\; ; \;\; N_R(\nu) = \hat{N}_R(\nu) + \frac{7}{72(4\pi)^2}$$

$$\hat{M}_R(\nu) = \frac{l_1^r(\nu)}{4} \;\; ; \;\; \hat{N}_R(\nu) = \frac{l_2^r(\nu)}{4}, \tag{3.5}$$

one gets typically $\hat{M}_R \sim -\hat{N}_R$ with negative $\hat{M}_R$ for QCD-like scenarios whereas a different region of $\hat{N}_R << \hat{M}_R$ with positive $\hat{M}_R$ is obtained for Higgs-like scenarios. Thus, for instance, in a Higgs-like scenario with $M_H = 2TeV$ and $\nu = 2TeV$ one gets: $\hat{N}_R = -9.7 \times 10^{-4}$ and $\hat{M}_R = 1.7 \times 10^{-3}$. In the QCD-like scenario with $N_{TC} = 3$ and $\nu = 2TeV$ that corresponds to $M_{\rho_{TC}} = 2TeV$ one obtains, in contrast, $\hat{N}_R = 1.2 \times 10^{-3}$ and $\hat{M}_R = -1.1 \times 10^{-3}$. The latter values are translated into the following values for the scale independent parameters of ref.[4] (in doing this translation a departure from the chiral limit is assumed): $\bar{l}_1 = -0.56$ and $\bar{l}_2 = 5.77$, that are compatible with the ones recently obtained in [19].

It is also interesting to compare the different patterns for the cross-section as a function of the energy in the various scenarios. The cross-section is obtained by inserting the ChPT-amplitudes of eq.(2.7) into the standard formula:

$$\sigma(V_1^L V_2^L \to V_3^L V_4^L) = \int_{-1}^{1} dcos\theta \frac{d\hat{\sigma}}{dcos\theta} \;\; ; \;\; \frac{d\hat{\sigma}}{dcos\theta} = \frac{|T(V_1^L V_2^L \to V_3^L V_4^L)|^2}{32\pi M_{VV}^2}. \tag{3.6}$$

For final states with identical particles an additional factor of $1/2$ must be included.

In fig.2 two typical cases have been displayed: Higgs-like with $M_H = 2TeV$ and QCD-like with $N_{TC} = 3$ ($M_{\rho_{TC}} = 2TeV$). The LET results are also shown for comparison. As expected, the Higgs-like curve lies always above the QCD-like curve in the $W^+W^- \to ZZ$ channel, whereas the contrary happens in the $W^\pm Z \to W^\pm Z$ channels. This fact is nothing else than the consequence of the presence of a low energy tail coming from either a scalar resonance or a vector resonance respectively.

4 SISBS signals at LHC and SSC

A typical signature of a SISBS at pp supercolliders will be an anomalous enhancement over the continuum background in the TeV region of the invariant mass distribution (M_{WW}) and the transverse momentum distribution (p_T^W) of the $pp \to (W_L W_L \to W_L W_L) + X$ events. These events are referred to in the literarure as $W_L W_L$-pair production by the WW-fusion mechanism. Of course, if the SBS is strongly interacting, in addition, an anomalous enhancement (as compared to the corresponding SM predictions with $M_H << 1TeV$) in multiple W_L production by the same WW-fusion mechanism is also expected (for some numerical estimates see last ref. of [7]). This would be the analogous one to multiple pion production in pion-pion scattering.

In order to compute the cross-section for the processes $pp \to (V_1^L V_2^L \to V_3^L V_4^L) + X$, we have used the effective W-approximation [20] that allows us to derive it in terms of the cross-section for the subprocess $V_1^L V_2^L \to V_3^L V_4^L$, where the initial longitudinal gauge bosons are taken to be real. More precisely, it is given by:

$$\sigma = \sum_{ij} \int\int d\tau d\eta f_i(x_1, Q^2) f_j(x_2, Q^2) \int\int d\hat{\tau} d\hat{\eta} (\frac{d^2\mathcal{L}}{d\hat{\tau} d\hat{\eta}})_{V_1 V_2} \times \hat{\sigma} \tag{4.1}$$

where f_i and f_j are the distribution functions of the quarks i and j, respectively, inside the proton; the variables τ and η are related to the momentum fractions of the quarks by $x_{1,2} = \sqrt{\tau} e^{\pm\eta}$; the variables $\hat{\tau}$ and $\hat{\eta}$ are related to the momentum fractions of V_1, V_2 with respect to q_i, q_j, $\hat{x}_1$ and $\hat{x}_2$, by $\hat{x}_{1,2} = \sqrt{\hat{\tau}} e^{\pm\hat{\eta}}$; $(\frac{d^2\mathcal{L}}{d\hat{\tau} d\hat{\eta}})$ is the luminosity function for the gauge boson pair $V_1^L V_2^L$ to be radiated from the quark pair $q_i q_j$ [20]; and $\hat{\sigma}$ is the cross-section for the subprocess $\hat{\sigma} = \sigma(V_1^L V_2^L \to V_3^L V_4^L)$ given in eq.(3.6).

In our search for typical signatures of a SISBS at LHC (and SSC) we have been systematic: 1) we have looked at the four different final states in pair boson production, W^+W^-, ZZ, $W^\pm Z$ and $W^\pm W^\pm$ and, 2) we have made predictions for the three characteristic scenarios: Scaled-QCD, $SU(N_{TC})$ Technicolour and a Higgs-like scenario. Notice, however, that our study could be extended to more exotic scenarios, such as for instance those containing a system with isospin and electric charge equal to two that would resonate in the W^+W^+ or W^-W^- channels. Finally, in order to be conservative we have considered just the leptonic decays of the final gauge bosons.

5 Some numerical results

For the numerical computations we have used the EHLQ structure functions set II [21] and the VEGAS MonteCarlo program for integration. The following parameters for LHC and SSC were assumed:

$$LHC, \sqrt{s} = 16TeV, L = 4 \times 10^{34} cm^{-2} sec^{-1}$$

$$SSC, \sqrt{s} = 40TeV, L = 10^{33} cm^{-2} sec^{-1}$$

All the numbers of events presented in this paper correspond to a running time of $10^7 sec$. An optimization procedure that enhances and optimizes the signal-to-background ratios

was also implemented in our programs. We will present here just a short summary of our numerical results. For a more detailed description of the signal and background processes as well as for more numerical predictions at LHC and SSC we address the reader to the LHC-Aachen-1990 Proceedings in ref.[7].

5.1 W^+W^- CHANNEL

This channel looks potentially very interesting in terms of signal rates and signal patterns as it would give resonant behaviour in all the three scenarios considered here. However, in view of the present lower bounds for the top quark mass, $m_t > 89\ GeV$ [22], already above the W-boson mass, it turns out that the dangerous background $pp \to t\bar{t}X$ with the top (anti-top) quarks decaying into real W^+'s (W^-'s) overwhelms completely the signal. In view of that we have not considered this channel here.

5.2 ZZ CHANNEL [7]

This channel offers a potential good probe for the Higgs-like scenario and in general for any scenario containing a scalar- isoscalar resonance. The reason is that it couples dominantly to the I=J=0 channel and therefore, in principle, it could produce either a bump or, in the worst case an enhancement in the invariant mass distribution of the gold-plated events, $l^+l^-l^+l^-$ with $l = \mu$ or e, over the continuum background. The results for this channel are collected in table 1 and fig.3.

From these numerical results one can conclude that the search for SISBS signals in this channel seems difficult. The signal-to -background ratio is always less than one and there is no prominent enough bump in the M_{ZZ}-invariant mass distribution. The most favourable case is the Higgs-like scenario where the best S/B-ratio for the $l^+l^-l^+l^-$ events that can be obtained at LHC with the highest luminosity is 33/75. The S/B-ratio at SSC is slightly larger (8/11) but it is poor in statistics. The results with the K-matrix method (not shown in table 1) give comparable signal rates for the Scaled-QCD scenario and sligthly smaller rates (about a factor 2/3) for the Higgs-like scenario.

The curves show a small enhancement in the high-M_{ZZ} region of the M_{ZZ}-invariant mass distribution over the continuum. This enhancement is clearly larger in the Higgs-like scenario than in the Scaled-QCD one and, in general, the corresponding total signal rates are in a ratio of 2 to 1 respectively. Finally, whether it will be possible to discern this small enhancement from the continuum or not is a question strongly dependent on the accuracy in the calibration of this continuum along the whole invariant mass range.

5.3 $W^\pm Z$ CHANNELS [7]

These channels are a good probe for the Scaled- QCD and Technicolour scenarios and, in general, for any scenario containing a ρ-like vector resonance (for instance the $V^\pm$ resonances of the BESS model [23]). This resonance couples dominantly to the I=J=1 channel and therefore can give rise to a resonant behaviour in $W^\pm Z$ production at LHC and SSC. The final $l^\pm\nu l^+l^-$ leptonic events (with $l = \mu$ or e) produced from the decay chain $\rho^\pm \to W^\pm Z \to l^\pm\nu l^+l^-$ will present typical signatures and distributions characterized by the physical parameters (the mass and the width) of this resonance.

Here we distinguish the Higgs-like scenario from the other ones. In the Higgs-like scenario there is just one type of signal process: 1) $W_L^\pm Z_L \to W_L^\pm Z_L$, whereas, in the Scaled-QCD and Technicolour scenarios there are two kind of processes that contribute to the signal, that is to $W_L^\pm Z_L$ production: 1) $W_L^\pm Z_L \to W_L^\pm Z_L$, and 2) $q\bar{q}' \to W^\pm \to \rho_{TC} \to W_L^\pm Z_L$. The first mechanism is the so-called WZ fusion process and gives a generic SISBS signal since it is present in all the SISBS scenarios. The second mechanism, where $q\bar{q}'$ annhilates into ρ_{TC} via $\rho_{TC} - W$ mixing, is not present in the Higgs- like scenario but it is always present in any SISBS scenario containing a vector resonance with the quantum numbers of the W gauge boson. This is, for instance, the case of the Scaled-QCD scenario, Technicolour and the BESS model [23]. For the two scenarios we are concerned with, we will assume as a reasonable working hypothesis that this second mechanism is well described in terms of Vector Meson Dominance (VMD) [21],[24].

The results for the signal-to-background ratios, S/B, of the final leptonic $l^\pm\nu l^+l^-$ events ($l = \mu$ or e) after applying the optimal cuts are collected in table 2. Predictions were made for the three scenarios: Scaled-QCD, Technicolor and the Higgs-like scenario. We have also computed the signal that would be produced in the Standard Model at tree level with a heavy Higgs boson of $m_H = 1TeV$ (SMH), in order to compare the results with our Higgs-like scenario results (HIGGS) that, in contrast, include the one-loop corrections and a unitarization procedure. In comparing the SMH and the Higgs- like scenario we find, as expected, comparable rates. The slight differences in the corresponding S/B ratios appearing in table 2 are due to the differences in the applied optimal cuts. As is clear from the results in table 2, the S/B ratios are too low to be observable in either the Higgs-like scenario or in the SMH.

The situation is completely different in the Scaled-QCD and Technicolour scenarios, where there are actual possibilities of observing the signal over the background with the total S/B ratios always being larger than one (see table 2). The contributions to the signal coming from the WZ fusion process and the $q\bar{q}'$ annhilation process via $\rho_{TC} - W$ mixing are presented separately in table 2. We would like to emphasize here that the S/B ratios obtained by considering just the WZ fusion contribution to the signal represent the most general and conservative expectations for the SISBS signals at LHC and SSC, and are already (for all the cases considered here) larger than one. The WZ fusion mechanism gives a generic SISBS signal and does not involve any assumption about the couplings between the fermionic sector and the SBS. The relative percentages of the WZ fusion contribution to the total signal are:

M_ρ	*rap.cut*	.....	$1.0TeV$	$1.5TeV$	$2.0TeV$
LHC	(2.5)	.....	9%	24%	45%
SSC	(2.5)	.....	22%	50%	72%

An increase in M_ρ results in a larger contribution from the WZ fusion process, which reveals itself as the most efficient mechanism in probing the SISBS for large enough values of M_ρ. This fact is clearly reflected in figures 4a and 4b. It is interesting to point out that the contribution of the fusion process is even more important at the SSC than at the LHC, due to the higher energy available at the subprocess level.

In figures 5a (LHC) and 5b (SSC) the M_{WZ} invariant mass distributions of the different background processes are displayed and for reference we have also included the spectrum of the WZ fusion signal process (with the optimal cuts).

As is clearly manifested in figures 4 and 5 and in table 2, the results are encouraging for both LHC and SSC and for all the three values of M_ρ considered. Special mention must be given to the technicolour models where there is a large and clear signal in the M_{WZ}

spectrum. In both cases, the Scaled-QCD and Technicolour scenarios, masses up to 2 TeV will be reachable at LHC.

5.4 $W^{\pm}W^{\pm}$ CHANNELS [25]

These channels are called exotic channels since they produce 2 like-sign leptons in the final state ($l^{\pm}\nu l^{\pm}\nu$ with $l = \mu$ or e) that are not easily produced by means of standard physics. Any potential signal in these channels will compete with a less prominent background than in the other channels. For instance, the important qq' background in W^+W^-, ZZ and $W^{\pm}Z$ channels is not present in $W^{\pm}W^{\pm}$ channels. Unfortunately, the $W^{\pm}W^{\pm}$ channels are not good probes for any of the scenarios considered here in the sense that these scenarios do not contain any doubly charged resonance with I=2 that could resonate in the $W^{\pm}W^{\pm}$ channels. However, it is precisely their singular nature that makes these channels more interesting, especially adequate for probing new unexpected resonances. For the scenarios we are concerned with, the expected SISBS signal will be an enhancement in the large invariant mass M_{WW} that, unfortunately, is hard to translate into physical leptonic variables. Concerning the background processes in these channels, they have been studied in detail by Barger et al. in [25]. In conclusion, these channels will serve at best as a test-confirmation of compatibility with whatever is seen in the ZZ and/or $W^{\pm}Z$ channels.

The results for the signal-to-background ratios, S/B, of the final $l^+\nu l^+\nu$ events ($l = \mu$ or e), for various choices of the invariant mass cut are shown in table 3. The corresponding rates for the $l^-\nu l^-\nu$ events (not shown in the table) are approximately 1/3 of those in table 3. The results from a tree-level calculation in the SM with a Higgs boson of $M_H = 1TeV$ (SMH) are also included for comparison with our Higgs-like scenario (HIGGS). From these numerical results one can conclude that the search for SISBS signals coming from the kind of scenarios considered in this talk will be very hard in these channels. The S/B ratio is always less than one and the M_{WW} distribution of the signal shows no singular behaviour. From figs. 6a and 6b it is clear that for the energy range of interest the total background is well above the signal. In ref.[25] it is claimed that by using central jet vetoing techniques one can notably improve the S/B ratios. Since the signal in this report is computed by means of the Effective W approximation, that assumes zero transverse momentum for the WW system and the remaining jet-jet system, these jet vetoing techniques cannot be implemented properly here. We leave this work for a Monte Carlo level simulation.

6 CONCLUSIONS

We have studied the V_LV_L scattering at LHC and SSC in the Chiral Lagrangian formalism that incorporates all the facts that are known about the symmetry breaking sector of the SM and has the appealing feature of treating the SISBS problem within a general framework (a feature always desirable, given the controversial nature of the subject). ChPT allows us to simulate different possible scenarios for the SISBS. We have presented in this talk some of the phenomenological implications at LHC and SSC of three of them: Scaled-QCD, Technicolour and a Higgs-like scenario. This study was done in a systematic way for the three relevant channels: ZZ, $W^{\pm}Z$ and $W^{\pm}W^{\pm}$, and, in order to be conservative, we have considered just the leptonic decays of the gauge bosons.

Our main conclusions can be summarized as follows:

1.- If the SBS behaves at the TeV energy scale like the Higgs-like scenario or like the Standard Model with a heavy Higgs boson of $M_H = 1TeV$, it will be difficult to disentangle any signal from the background at LHC (and SSC). The most favourable channel is ZZ, where a small enhancement in the O(1TeV) M_{ZZ} region of the spectrum of the gold-plated events is found. The S/B ratios are always less than one and there is a lack of statistics in the signal. The best ratio found is S/B = 33/75 and it corresponds to the highest integrated luminosity option for LHC of $L = 4 \times 10^5 pb^{-1}$.

2.- If the SBS behaves at the TeV energy scale like the Scaled-QCD or Technicolour scenarios, characterized by the existence of a ρ-like vector resonance, there are actual possibilities of observing the signal over the backround in the $W^{\pm}Z$ channels. A clear resonance shape will show up in the M_{WZ} and p_T^Z spectra. If the highest luminosity option for LHC is achieved, masses up to $M_\rho \sim 2TeV$ will be tested. The WZ fusion mechanism contributes about 50% (70%) to the total signal at LHC (SSC) for $M_\rho = 2TeV$. It will provide by itself generic SISBS signals that involve just the interactions in the SBS and not the interactions of the SBS with the fermionic sector.

For ρ-like particles lighter than $2TeV$ ($1.5TeV$), the qq' annhilation mechanism, where qq' annhilates into ρ via $\rho - W$ mixing, starts being the dominant one at LHC (SSC). The rates computed with the VMD assumption show that there will be sizeable S/B ratios with also sizeable statistical significance (see table 2).

3.- No clear SISBS signal is found in the $W^{\pm}W^{\pm}$ channels for any of the three scenarios studied here. However, this channel offers itself as an ideal laboratory to search for new exotic resonances.

Acknowledgements

I would like to thank my colleagues Antonio Dobado and Juan Terron with whom most of the work reported in this talk was carried out.

References

[1] D.A.Dicus and V.Marthur, Phys.Rev. **D7**(1973)3111; J.M. Cornwall,D. N. Levin and G. Tiktopoulos, Phys. Rev. **D10** (1974)1145; B. W. Lee, C. Quigg and H. Thacker, Phys. Rev. **D16**(1977)1519; M. Veltman, Acta Phys. Pol. **B8**(1977)475; M. S. Chanowitz and M. K. Gaillard, Nucl. Phys. **B261**(1985)379.

[2] R.N.Cahn and S.Dawson, Phys.Lett.**136B**(1984)196; **138B**(E)(1984)464.

[3] For a recent review of the field and many further references see M. S. Chanowitz, Ann. Rev. Nucl. Part. Sci. **38**(1988)323.

[4] S. Weinberg, Physica **96 A**(1979)327; J. Gasser and H. Leutwyler, Ann. of Phys. **158**(1984)142.

[5] A.Dobado and M.J. Herrero, Phys.Lett.**B228**(1989)495; **B233**(1989)505; J.F.Donoghue and C.Ramirez, Phys.Lett.**B234**(1990)361.

[6] T.N.Truong, Phys.Rev.Lett. **61**(1988)2526; A.Dobado, M.J.Herrero and T.N.Truong, Phys.Lett.**B235** (1990)129, and 134.

[7] A. Dobado, M.J. Herrero and J. Terron, CERN preprint CERN-TH.5670/90, to appear in Z. Phys. C (1991); A. Dobado, M.J. Herrero and J. Terron, CERN preprint CERN-TH.5813/90, to appear in Z. Phys.C (1991); A. Dobado, M.J. Herrero and J. Terron, CERN preprint CERN-TH.5959/90, to appear in Proceedings of the ECFA-LHC Workshop, Aachen, October 1990.

[8] S.Dawson and G.Valencia, preprint BNL-45194, to appear in Nucl.Phys.B(1990); J.Bagger, S.Dawson and G.Valencia, CERN preprint CERN-TH.5989/90.

[9] A.Dobado, D.Espriu, M.J.Herrero, CERN preprint CERN-TH.5785/90, to appear in Phys.Lett.B(1991).

[10] M. Chanowitz, M. Golden and H. Georgi, Phys. Rev. **D36**(1987)1490.

[11] E.Farhi and L.Susskind, Phys.Rep.**74**(1981)277; S.Dimopoulos and L.Susskind, Nucl.Phys.**B155**(1979)237.

[12] K.Kawarabayashy and M.Suzuki, Phys.Rev.**16B**(1966)225; Riazuddin and Fayazuddin, Phys.Rev.**147**(1966)1071.

[13] A. Dobado, M.J. Herrero and T.N. Truong, Phys.Lett. **B235** (1990)129.

[14] S.Dawson and S.Willenbrock, Phys.Rev.**D40**(1989)2880; M.Veltman and F.J.Yndurain, Nucl.Phys. **B325** (1989)1. A one-loop computation of the logarithmic terms was previously made in an effective Lagrangian approach in: O.Cheyette and M.K.Gaillard, Phys.Lett.**B197**(1987)205.

[15] The problem of unitarization in LWB scattering has been discussed recently by a number of authors: O.Cheyette and M.K.Gaillard in [14]. D.A.Dicus and W.Repko, Phys. Lett.**B228**(1989)503; S. Dawson and S. Willenbrock, Phys. Rev. Lett. **62** (1989) 1232; A.Dobado et al. in [5], [6] and [7]; D.A. Dicus and W.W. Repko, preprint MSUTH 89/06; R.Rosenfeld, preprint EFI-89-54.

[16] A.Dobado et al. in [6].

[17] A.Dobado, Phys.Lett. **B237** (1990) 457; S.Willenbrock, preprint BNL-44955 (1990).

[18] M.B.Einhorn, Nucl.Phys.**B246** (1984)75; R.Casalbuoni, R.Dominici and R.Gatto, Phys.Lett. **147B**(1984)419. See also Lee et al. in [1].

[19] C.Riggenbach et al., CERN preprint CERN-TH.5755/90.

[20] S. Dawson, Nucl. Phys. **B249**(1985)42.

[21] E.Eichten et al., Rev.Mod.Phys.**56**(1984)579.

[22] CDF collaboration, F.Abe et al., Phys.Rev.Lett.**64**(1990)142.

[23] R.Casalbuoni et al., Phys.Lett.**B249**(1990)130.

[24] J.J. Sakurai, *Currents and Mesons*, University of Chicago Press,1969; R. Rosenfeld and J.L. Rosner, Phys. Rev.**D38** (1988)1530; R.S. Chivukula, preprint BUHEP-88-16.

[25] V.Barger et al., Phys.Rev.**D42**(1990)3052; J.Terron, Ph.D. Thesis (presented at the Univ. Autonoma de Madrid, October 1990) unpublished; D.A.Dicus, J.F.Gunion, R.Vega, SLAC preprint SLAC-PUB-5407/1990.

Figure Captions

Fig. 1: Position in the parameter space $(N_R(\nu), M_R(\nu))$ of the three scenarios discussed in this paper: Higgs-like, Scaled-QCD and Technicolour. The two latter are named together QCD-like in this plot. The following choices were made: $\nu = 2, 1, 1.5TeV$; $M_H = 1, 1.1, 1.2, ..., 2, 3, ...10TeV$; $N_{TC} = 3, 4, ..., 12$.

Fig. 2: Cross-sections for Longitudinal Weak Boson scattering in ChPT to $O(s^2)$ as a function of the energy. The dot-dashed lines correspond to a Higgs-like scenario with $M_H = 2TeV$. The dashed lines correspond to the Scaled-QCD scenario where $N_{TC} = 3$ or, equivalently, $M_{\rho_{TC}} = 2TeV$. The predictions from ChPT to lowest order, that is, the LET results, are also plotted for comparison (solid lines).

Fig. 3: ZZ-events distribution with respect to the invariant mass M_{ZZ} for SISBS signals at LHC. No leptonic BR has been included. The top mass value chosen is $m_t = 100GeV$. The LWB scattering amplitudes were unitarized with the Pade method. Solid histograms are the total rates, signal plus background. Dashed histograms are the background contribution alone. (a) Predictions for the Higgs-like scenario. (b) Predictions for the Scaled-QCD scenario.

Fig. 4: (a) WZ invariant mass distribution of the signal and background processes with the optimal cuts for the LHC (a 2.5 rapidity cut has been chosen for the final weak bosons). No leptonic BR has been included. The results for the Scaled-QCD and Technicolour scenarios are displayed: lower solid histogram represents WZ fusion signal process and dotted histogram represents qq' annihilation signal process. The total background is the dashed histogram and the total background plus total signal is the upper solid histogram. (b) Same for the SSC.

Fig. 5: (a) WZ invariant mass distribution for the WZ fusion signal process (solid histogram) and for the background processes (dashed histogram for qq', dotted histogram for γ W fusion and dash-dotted histogram for $W_T Z_T$ fusion background process). of the Scaled-QCD scenario for the LHC (the 2.5 rapidity cut has been chosen). No leptonic BR has been included. (b) Same for the SSC.

Fig. 6: Like-sign WW invariant mass distribution for the various SISBS scenarios and for the total background. Rates are for $W^+W^+ + W^-W^-$. No leptonic BR has been included. The short-dashed line is for the Scaled-QCD scenario and the lower solid line is for the Higgs-like scenario. The upper solid curve corresponds to the unitarized Low Energy Theorems results taken from [25]. The SM rates for $M_H = 1TeV$ (SMH) are also shown for comparison (dot-dashed line). The long dashed lines are the results for the total background taken from [25]. The upper line is for $m_t = 100GeV$. The lower line is for $m_t = 200GeV$.

Table Captions

Table 1: ZZ channel: Number of $l^+l^-l^+l^-$ events for SISBS signals in two scenarios, and for the total background. Rates are presented in the form of S/B-ratios for both LHC and SSC. Two different rapidity cuts, 1.5 and 2.5, and two values of the top quark mass were chosen. The numbers in parenthesis are the optimal cuts, (P_Z^T, M_{ZZ}) in GeV.

Table 2: WZ channel: Number of $l^+\nu l^+l^- + l^-\nu l^+l^-$ events for the total SISBS signal in various scenarios and for the total background at LHC and SSC. Rates are presented in the form of S/B-ratios. The rates for both processes contributing to the signal in Scaled-QCD and Technicolour scenarios: WZ-fusion (WZ) and qq' annhilation (qq') are also shown separately for comparison. The optimal cuts in GeV are shown in parenthesis as (P_Z^T) or (P_Z^T, M_{WZ}) depending on the case.

Table 3: W^+W^+ channel: Number of $l^+\nu l^+\nu$ events for SISBS signals in various scenarios at LHC and SSC. Rates are presented in the form of S/B-ratios.

Table 1: ZZ channel

Scenario	LHC (1.5) $m_t = 100GeV$	LHC (2.5) $m_t = 100GeV$	SSC (1.5) $m_t = 100GeV$	SSC (2.5) $m_t = 100GeV$
HIGGS	27/48 (300,750)	33/75 (300,750)	5/6 (240,750)	8/11 (240,750)
QCD	9/36 (360,750)	15/90 (300,700)	2/3 (360,800)	3/6 (360,800)
	LHC (1.5) $m_t = 180GeV$	LHC (2.5) $m_t = 180GeV$	SSC (1.5) $m_t = 180GeV$	SSC (2.5) $m_t = 180GeV$
HIGGS	25/57 (300,750)	39/111 (240,750)	5/8 (240,750)	8/14 (240,750)
QCD	12/69 (300,700)	15/102 (300,700)	2/6 (300,800)	3/12 (300,750)

Table 2: WZ channel

Scenario	LHC (1.5)	LHC (2.5)	SSC (1.5)	SSC (2.5)
TECHN 1.0	1713/71 161 (WZ) 1552 ($q\bar{q}'$) (10)	2628/213 318 (WZ) 2310 ($q\bar{q}'$) (180)	142/7 26 (WZ) 116 ($q\bar{q}'$) (10)	263/24 59 (WZ) 204 ($q\bar{q}'$) (180)
TECHN 1.5	136/16 33 (WZ) 103 ($q\bar{q}'$) (360)	197/43 59 (WZ) 138 ($q\bar{q}'$) (300)	18/2 8 (WZ) 10 ($q\bar{q}'$) (300)	33/6 17 (WZ) 16 ($q\bar{q}'$) (300)
QCD 2.0	53/25 23 (WZ) 30 ($q\bar{q}'$) (480)	65/31 29 (WZ) 36 ($q\bar{q}'$) (540)	11/4 7 (WZ) 4 ($q\bar{q}'$) (480)	21/12 15 (WZ) 6 ($q\bar{q}'$) (420)
HIGGS	20/434 (300,500)	27/786 (300,500)	3/17 (420,500)	5/34 (420,500)
SMH	29/907 (240,500)	39/1744 (240,500)	5/87 (240,500)	7/196 (240,500)

Table 3: WW channel

$m_t = 100GeV$	LHC (1.5)			SSC (1.5)		
Scenario	$M_{WW} > 0.8TeV$	1.0TeV	1.2TeV	$M_{WW} > 0.8TeV$	1.0TeV	1.2TeV
QCD	32/212	20/96	12/150	8/26	5/14	4/8
HIGGS	22/212	13/96	7/50	5/26	3/14	2/8
SMH	30/212	16/96	9/50	6/26	4/14	2/8
$m_t = 200GeV$	LHC (1.5)			SSC (1.5)		
Scenario	$M_{WW} > 0.8TeV$	1.0TeV	1.2TeV	$M_{WW} > 0.8TeV$	1.0TeV	1.2TeV
QCD	32/154	20/71	12/38	8/21	5/11	4/7
HIGGS	22/154	13/71	7/38	5/21	3/11	2/7
SMH	30/154	16/71	9/38	6/21	4/11	2/7

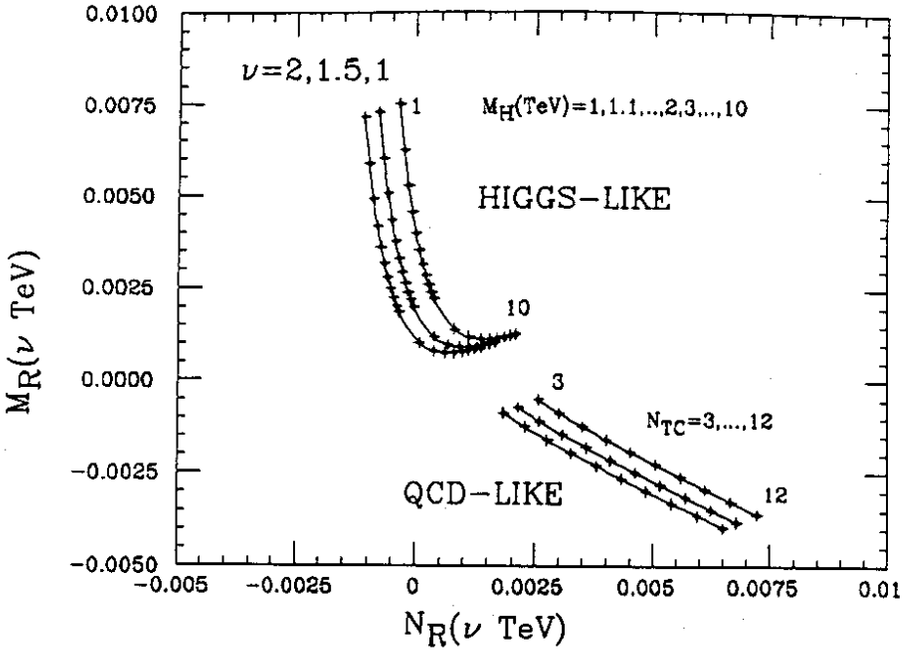

Figure 1

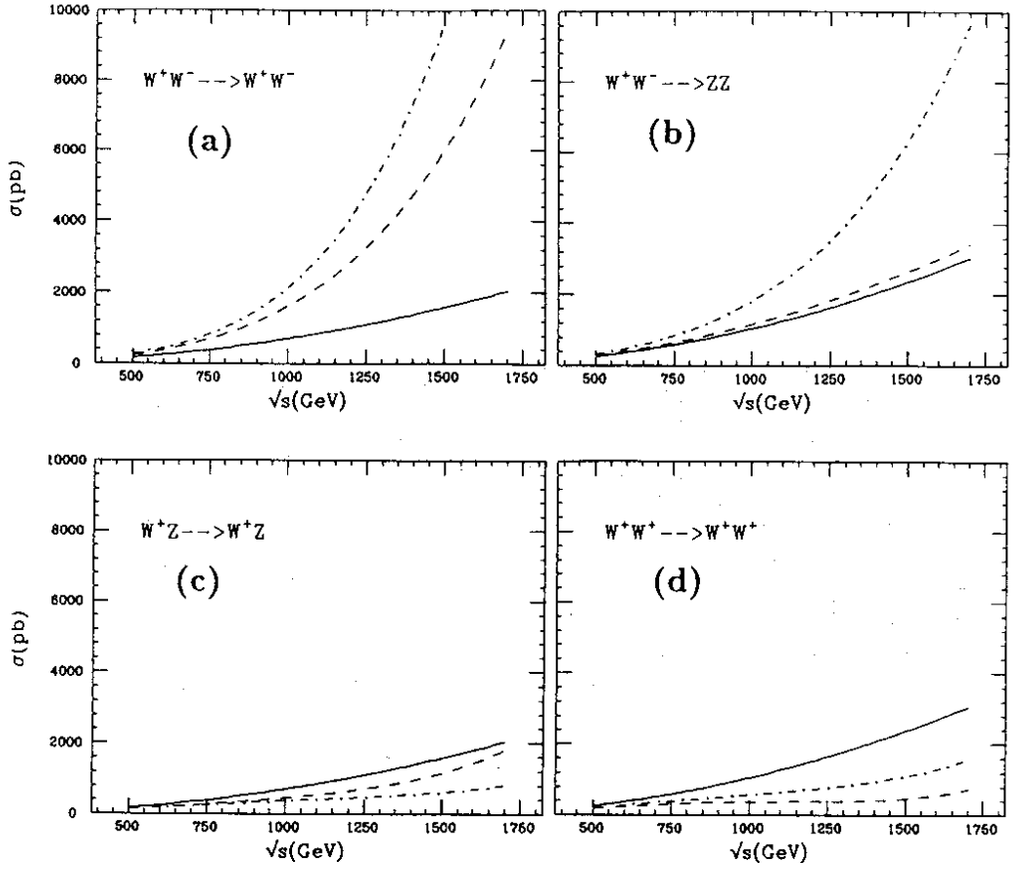

Figure 2

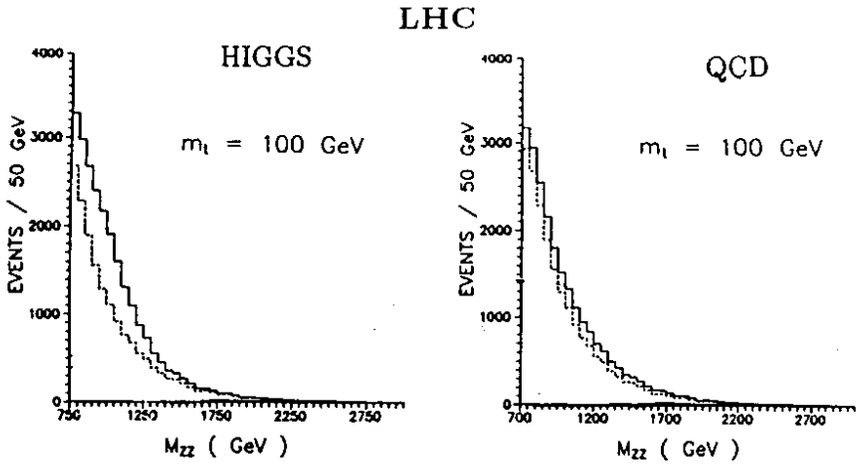

Figure 3

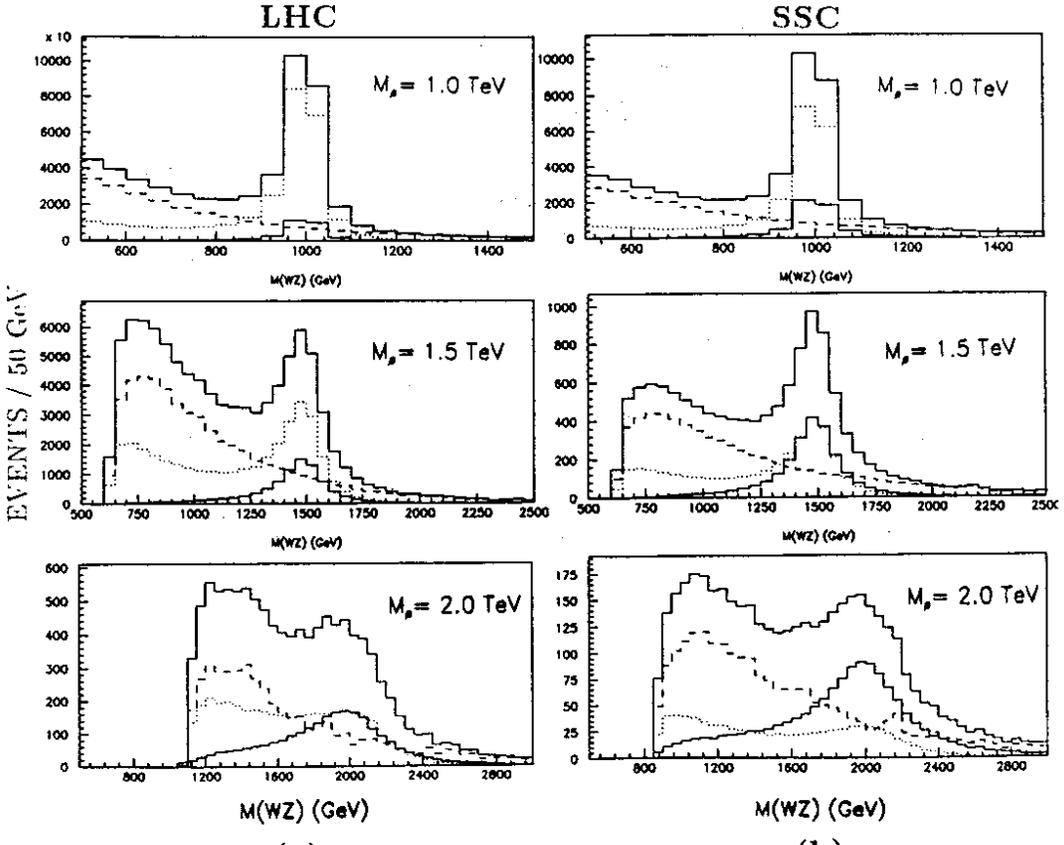

Figure 4

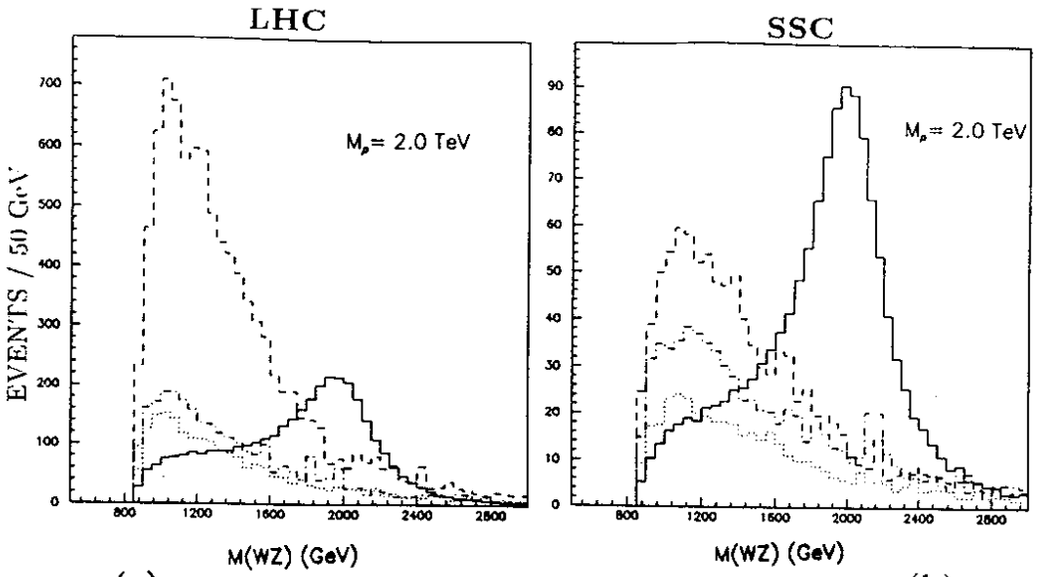

Figure 5

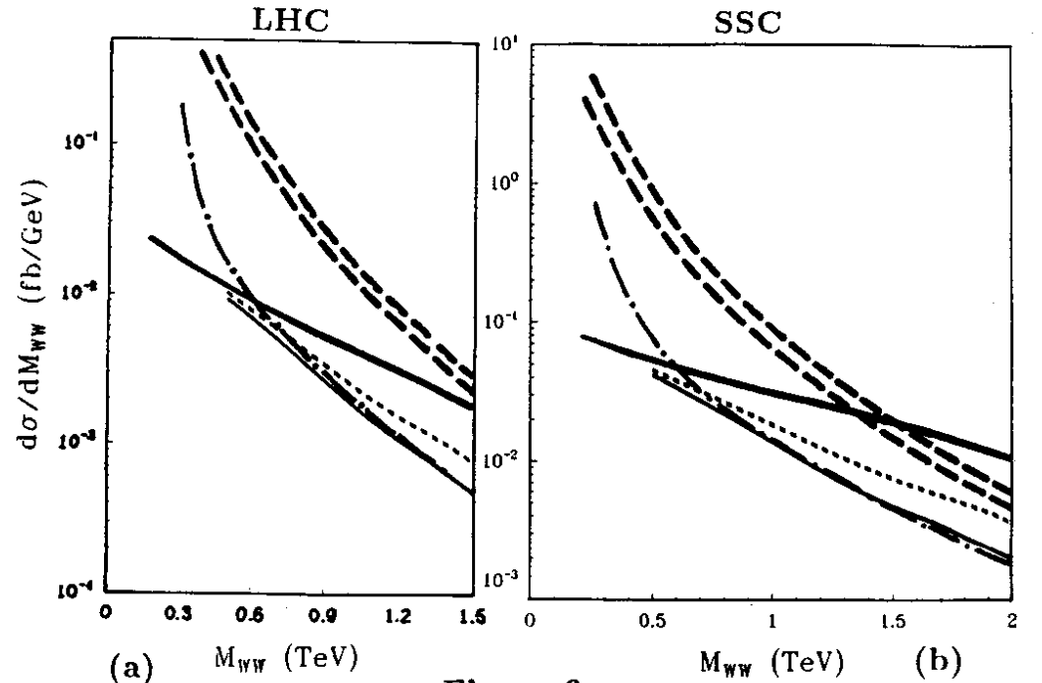

Figure 6

Imprimé au CERN. Prix : 0.40 Fr.